



RESEARCH ARTICLE

10.1029/2020JD034252

Key Points:

- Detailed distributions of needle properties are presented
- Possible physics behind needle production is discussed
- Recoil leaders quench needle activity

Correspondence to:






B. M. Hare,
B.H.Hare@rug.nl

Citation:

Hare, B. M., Scholten, O., Dwyer, J., Strepka, C., Buitink, S., Corstanje, A., et al. (2021). Needle propagation and twinkling characteristics. *Journal of Geophysical Research: Atmospheres*, 126, e2020JD034252. <https://doi.org/10.1029/2020JD034252>

Received 13 NOV 2020
Accepted 17 FEB 2021

Needle Propagation and Twinkling Characteristics

B. M. Hare¹ , O. Scholten^{1,2} , J. Dwyer³ , C. Strepka³, S. Buitink^{4,5}, A. Corstanje^{4,5}, H. Falcke^{4,6,7}, J. R. Hörandel^{4,5,6}, T. Huege^{5,8}, G. K. Krampah⁵, P. Mitra⁵, K. Mulrey⁵, A. Nelles^{9,10}, H. Pandya⁵ , J. P. Rachen⁵, S. Thoudam¹¹, T. N. G. Trinh¹² , S. ter Veen^{4,7}, and T. Winchen¹³

¹Faculty of Science and Engineering, Kapteyn Astronomical Institute, University of Groningen, Groningen, The Netherlands, ²Interuniversity Institute for High-Energy, Vrije Universiteit Brussel, Brussels, Belgium, ³Department of Physics and Astronomy, University of New Hampshire, Durham, NH, USA, ⁴Department of Astrophysics/IMAPP, Radboud University Nijmegen, Nijmegen, The Netherlands, ⁵Department of Physics, Astrophysical Institute, Vrije Universiteit Brussel, Brussels, Belgium, ⁶NIKHEF, Science Park Amsterdam, Amsterdam, The Netherlands, ⁷Netherlands Institute of Radio Astronomy (ASTRON), Dwingeloo, The Netherlands, ⁸Institute for Astroparticle Physics (IAP), Karlsruhe Institute of Technology (KIT), Karlsruhe, Germany, ⁹DESY, Zeuthen, Germany, ¹⁰ECAP, Friedrich-Alexander-University Erlangen-Nrnberg, Erlangen, Germany, ¹¹Department of Physics, Khalifa University, Abu Dhabi, United Arab Emirates, ¹²Department of Physics, School of Education, Can Tho University Campus II, Can Tho City, Vietnam, ¹³Max-Planck-Institut für Radioastronomie, Bonn, Germany

Abstract Recently, a new lightning phenomena, termed needles, has been observed in both VHF and in optical along positive lightning leaders. They appear as small (<100 m) leader branches that undergo dielectric breakdown at regular intervals (called twinkles). Providing a coherent and consistent explanation for this phenomenon is challenging as each twinkle is a form of negative breakdown that propagates away from the positive leader. In this study, we provide detailed observations of needles in VHF, observed during two lightning flashes. We show distributions of different needle properties, including twinkle propagation speeds, time between twinkles, and needle lengths, among others. We show a return stroke and multiple recoil leaders that quench needle activity. We also show that nearby needle activity does not seem to correlate together, and that needle twinkling can slow down by 10%–30% per twinkle. We conclude by presenting possibilities for how the positive leader could induce negative propagation away from the positive channel, and we argue that twinkles can propagate like a stepped leader or like a recoil leader depending on the temperature of the needle, which implies that needle twinkles can probably propagate without emitting VHF.

1. Introduction

Needles are a very recently discovered lightning phenomenon, described in Hare et al. (2019), that occur along positive leader channels. They appear like small leader branches, at most around 100-m long, and stick out from the channel. However, unlike leader branches, they exhibit ionization fronts that propagate up each needle, away from the positive leader channel. Hare et al. (2019) referred to these fronts as twinkles, and they occur at a very regular rate, around once per 5 ms. Pu and Cummer (2019) confirmed these findings, and showed that there is a location on the positive leader channel that moves forward along the positive at a regular speed ($\approx 10^5$ m/s), where there is no needle activity ahead of this point, and copious needle activity behind it. We call this point the needle production head (since it is the tip of where needles are produced), and we discuss it in more detail in Section 2.5.

Paradoxically, despite propagating away from the positive leader channel, Hare et al. (2019) concluded that since needles emit copious VHF while positive leaders do not (Edens et al., 2012; Hare et al., 2019; Shao et al., 1999), needle twinkles must thus be a form of negative propagation. Pu and Cummer (2019) confirmed this by showing that the negatively charged end of a bidirectional leader suppressed needle activity, and by showing a needle that extended into a full negative leader.

Saba et al. (2020) was able to observe optical emissions from needles on upward positive leaders. Saba et al. (2020) showed that these needles observed in optical had very similar properties to those reported in Hare et al. (2019) and Pu and Cummer (2019), including that they twinkled multiple times with a few milliseconds between twinkles without growing in length. However, the needles observed by Saba

© 2021. The Authors.

This is an open access article under the terms of the [Creative Commons Attribution-NonCommercial License](https://creativecommons.org/licenses/by-nc/4.0/), which permits use, distribution and reproduction in any medium, provided the original work is properly cited and is not used for commercial purposes.

et al. (2020) were somewhat shorter than those observed in Hare et al. (2019) and Pu and Cummer (2019). Saba et al. (2020) was even able to show that propagation of one 73-m long needle was away from the positive leader with a speed of about 2.7×10^5 m/s, and that a negative leader developed from the location of a needle, consistent with Hare et al. (2019) and Pu and Cummer (2019), and Saba et al. (2020) was able to confirm a hypothesis proposed by Hare et al. (2019), that the first needle twinkle occurs about 100 m or so behind the tip of the positive leader. Finally, Saba et al. (2020) was also able to show that needles are the result of a corona-brush split, which is where the corona in front of a positive leader splits into two different sections in a failed attempt to branch.

In this study, we present observations of typical needle behavior during two lightning flashes, including statistics on their lengths, twinkling rates, propagation speeds, and more. Among others, we show that: needle twinkles can potentially propagate without emitting VHF radiation, have a wide range of propagation speeds varying from stepped leaders up to dart leaders, and that needles cease twinkling after recoil leaders. In Section 2, we introduce the two flashes used in this study. In Section 2.1, we discuss a needle from each flash in detail. In Section 2.2, we give detailed statistics for many needles. In Section 2.3, we explore the relationship between negative leader and needles, and in Section 2.4, we explore the relation between recoil leaders and needles. In Section 2.5, we discuss the broader structure of needle activity on the positive leader. Finally, in Section 3, we discuss the possible physics behind needle twinkling and propagation.

2. Data

In this study, we use two flashes observed by the Low Frequency ARray (LOFAR) (van Haarlem et al., 2013). For consistency we use the same flash presented in Hare et al. (2019), which was observed on September 29, 2017 at 20:22:55 UTC. This 2017 flash occurred about 19 km from the LOFAR core and had a single negative return stroke about 73 ms after initiation and a failed dart leader about 200 ms after initiation. For comparison we also include data from an intracloud flash that occurred on April 24, 2019 at 19:44:32 UTC. We observed multiple flashes on this day, in this study, we focus on one flash in particular, chosen because it occurred 26 km from the LOFAR core (close enough that we have meter-scale accuracy, but not so close that the confusion limit becomes too large). The images for both flashes are shown in Figure 1.

Both of these flashes were imaged using a new algorithm that is improved over the one used in Hare et al. (2019), as it is significantly faster and locates around three times more sources. This new algorithm was inspired by Kalman-filters and is described in Scholten et al. (2020).

2.1. Specific Examples

Figure 2 shows two needles, one from each flash, that show the general characteristics of needles. For these two examples we purposely choose needles that are particularly long, as it is easier to demonstrate their important features. Furthermore, the needle from 2017 was also featured in Hare et al. (2019); however, here, we see more detail due to the improved imaging procedure.

Figure 2 shows a straight line that has been fitted to the VHF source locations of the needle shown in Figure 2, which we call the axis of the needle. In Section 2.2, we fit this axis to a large number of needles in order to extract distributions of length, speed, and other characteristics. This fitting was done by modeling each twinkle as a point that moved forward along the axis. We call this point the “twinkle tip.” For each needle, the input fitting parameters to the model were the location and direction of the axis and the speed of each twinkle. The location and direction of the axis were assumed to be the same for every twinkle, but the speed was allowed to be different, and each twinkle was allowed to have a different start location along the axis. Thus, there were five parameters for the axis location and direction, and two for each twinkle. These parameters were fitted such that, for each VHF source location on each twinkle, the distance between the twinkle tip (at the time of the VHF source) and the VHF source was minimized, using a Levenberg-Marquardt optimizer.

In the distance along axis versus time panel of Figure 2 each twinkle of the two needles appears as a vertical bar since the duration of each twinkle is much shorter than the time between twinkles. Each needle twinkles multiple times, with the time between twinkles generally around 5–10 ms. It is clear that the needles

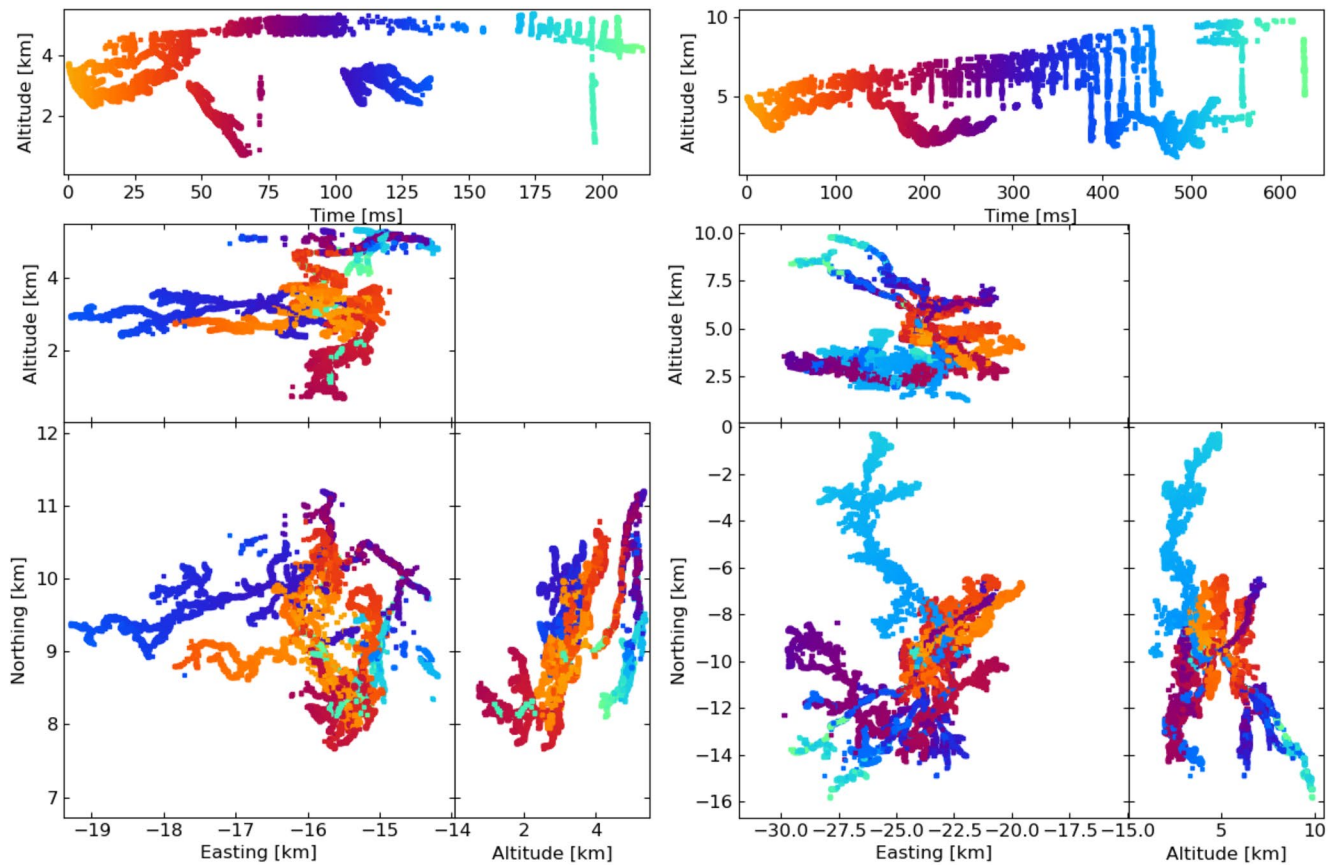


Figure 1. The images of the two lightning flashes used in this study. The 2017 flash is on the left, and the 2019 flash is on the right. Both of these flashes propagate into the main negative charge and the lower positive charge. Thus, each flash has two layers. The 2017 flash connects to ground and produces a return stroke at about 72 ms.

are not perfectly straight, they tend to curve, and each twinkle follows the same curved path. Furthermore, each twinkle does not extend the needle but also does not necessarily produce mappable VHF emission over the entire needle.

Figure 3 shows a zoom-in on a twinkle with many VHF sources from the two needles shown in Figure 2 at $T = 77$ ms and $T = 259$ ms from the 2017 and 2019 flashes, respectively. These two twinkles propagate at about 5.3×10^5 and 9.2×10^5 m/s on average, respectively, away from the positive leader. It is interesting to compare these two twinkles to the one at about $T = 56$ ms in the 2017 needle in Figure 2, which simply consists of two clusters of sources at the base and tip of the 2017 needle, 86 m and $5.6 \mu\text{s}$ apart, thus propagating at a speed of 1.5×10^7 m/s, 30 times faster than the twinkles featured in Figure 3. Both of the twinkles shown in Figure 3, however, seem to start with a fast propagation and then slow down. We have observed many twinkles that slow down (such as these two), and many that seem to have a constant speed.

2.2. Statistical Characteristics

Figure 4 shows a distribution of number of twinkles per needle and Figure 5 shows the distribution of time between twinkles per needle. These statistics were formed by choosing needles that could clearly be distinguished from other lightning structures (such as recoil leaders and other needles) using rectangular cuts in space and time, and twinkled at least twice, where a twinkle could consist of a single VHF source. The twinkles inside of each needle were separated when two subsequent VHF sources inside the same needle were greater than 0.5 ms apart. We verified by eye that this cut produces good results for all needles used in this study. It is possible that these distributions are affected by imaging inefficiencies, as some twinkles emit

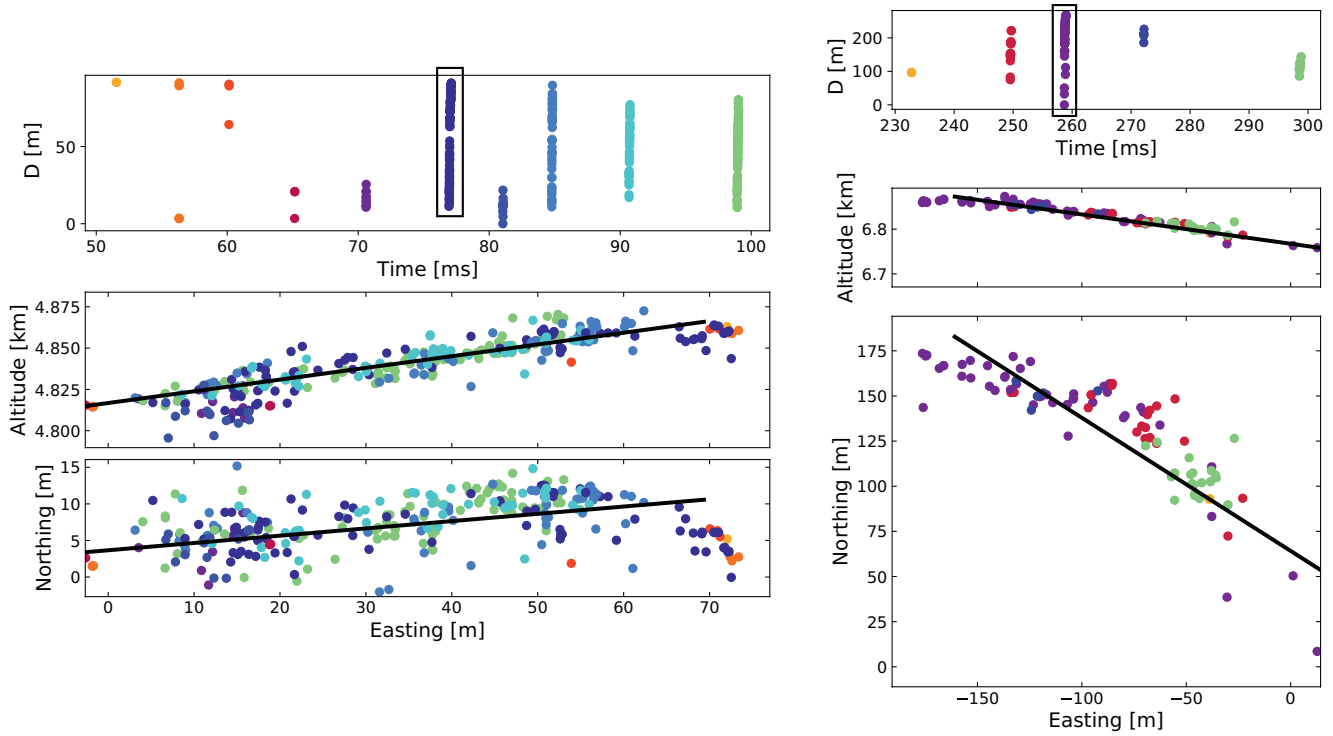


Figure 2. Examples of two needles. Black line shows the fitted axis. D is distance parallel to the axis. The origin (easting = 0, northing = 0) has been shifted relative to Figure 1. In this figure, the origin for the 2017 twinkle corresponds to $(-15.3, 10.32)$ km and the origin of the 2019 twinkle corresponds to $(25.5, -11.225)$ km, in Figure 1. The rectangles in D versus T indicate the twinkles features in Figure 3. The left is 2017, right is 2019 flashes.

very little VHF radiation (such as the first twinkle in the featured 2017 needle) and could be easily missed during imaging.

Figure 4 shows that the number of twinkles per needle follows a roughly uniform distribution, that there isn't one preferred number of twinkles. Figure 4 also shows that the maximum number of twinkles per needle is smaller in the 2019 flash than the 2017 flash. It is not clear if this is physical or due to imaging artifacts. Figure 5 shows that the time between twinkles tends to be between 2 and 7 ms. Large measured time between twinkles, especially larger than 10 ms, is most likely due to twinkles that were missed by the imaging.

The time between twinkles is very regular, as opposed to a random rate. Figure 6 shows the ratio of times between subsequent twinkles, that is, if a needle has three twinkles, A, B, and C, and T_{AB} and T_{BC} is the time between twinkles A, B and B, C, respectively, the distribution of T_{AB}/T_{BC} is shown in Figure 6. Figure 6 also shows the results of a simple Monte Carlo simulation that demonstrates how the results would appear if twinkling times were uncorrelated. This simulation was performed by simply sampling two values (with replacement) from the distribution of twinkling times, shown in Figure 5, and taking their ratio. The difference between this simulation and the data demonstrates the strength of the correlation between subsequent twinkles.

There is a question of whether needles twinkle at a constant rate, or slow down. Saba et al. (2020) observed in optical that the time between subsequent twinkles tends to increase. In order to explore this, we fitted the time of observed twinkles (T_i) with a simple model

$$T_i = T_0 + i \times \Delta T \times f^{i-1}, \quad (1)$$

that has three parameters. T_0 is the time of the first twinkle. ΔT is the time between first two twinkles, and f is the twinkle-time increase factor. The twinkle-time increase factor determined if the time between twinkles was constant (if the best-fit f was 1), or increase over time (if the best-fit f is greater than 1). For each of the same set of needles used to generate the other distributions in this study, we fitted this model to

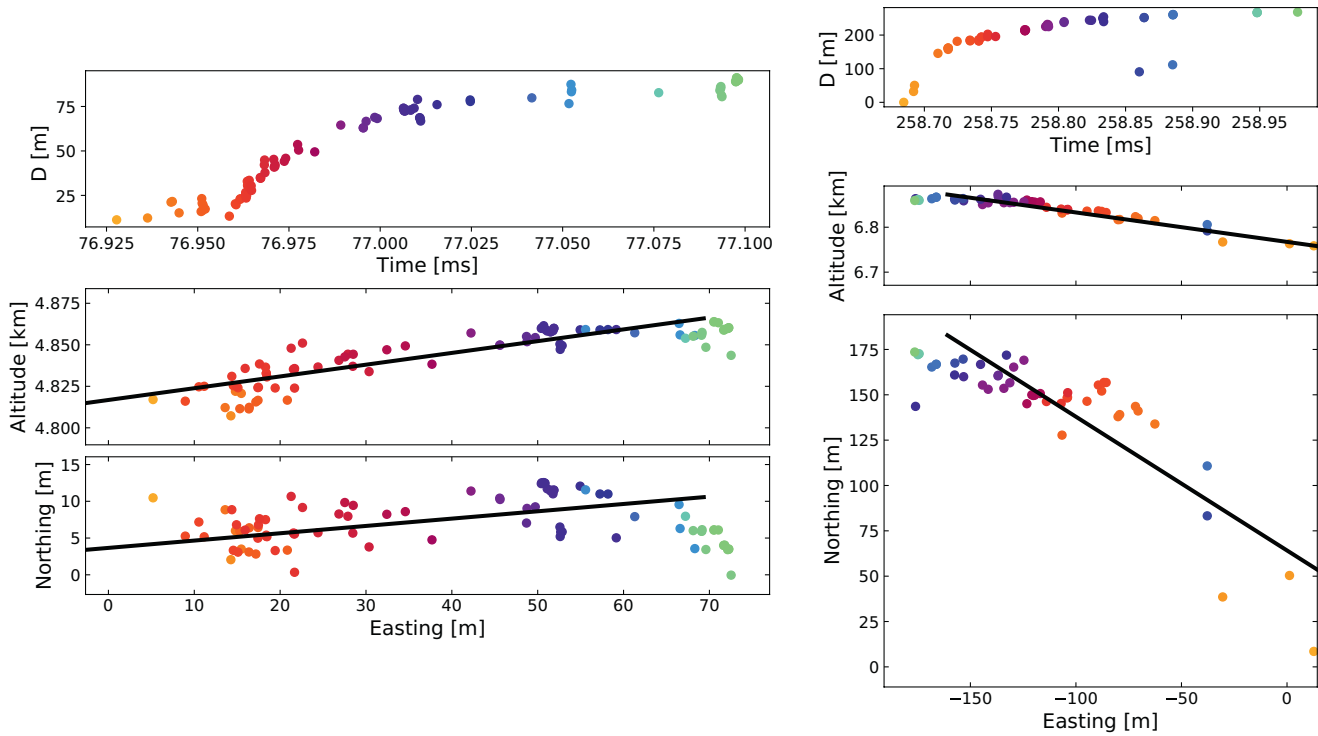


Figure 3. Examples of twinkles, in the needle shown in Figure 2. Left is 2017, right is 2019 flashes.

measured twinkle times using a Levenberg-Marquardt chi-square minimizer. For calculating the chi-square value, we used 5% of the time between twinkles as the twinkle-time error. We regularly miss twinkles from needles, which is easy to identify by eye when the separation between two twinkles is twice that between other twinkles in the same needle. Thus, if very few twinkles were missed by our imaging, and it was clear by eye which twinkles were missed, we allowed the model to include additional unimaged twinkles as chosen by eye. However, if too many twinkles were missed by our imaging then that needle was excluded from fitting. The precise criterion used was that the number of unimaged twinkles must be less than or equal to $N_{ot} - 4$, where N_{ot} is the number of observed twinkles. In addition, negative leaders, recoil leaders, and the return stroke in the 2017 flash, affect needle activity (discussed in more detail in later sections). In this fitting, we ignore the possible affects of negative leaders and recoil leaders. However, for the 2017 flash, we

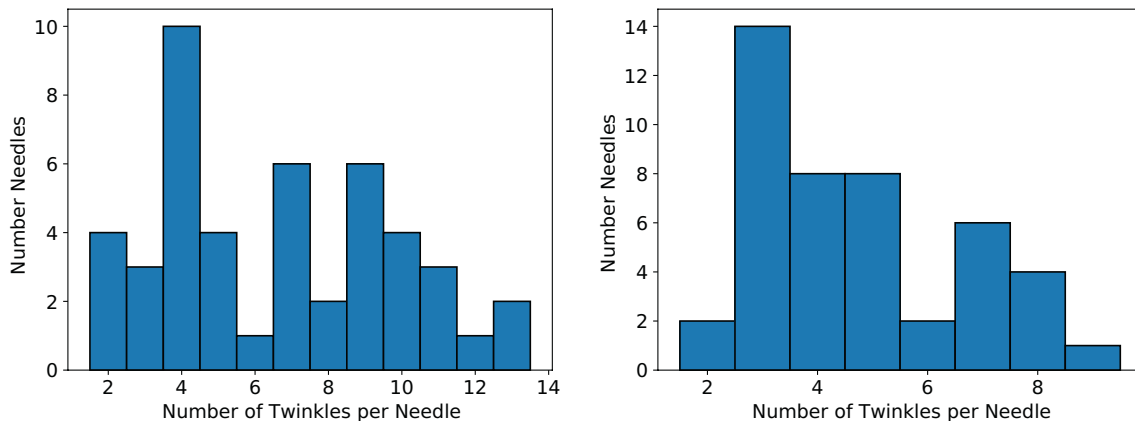


Figure 4. Number of twinkles per needle. Left is 2017, right is 2019 flashes.

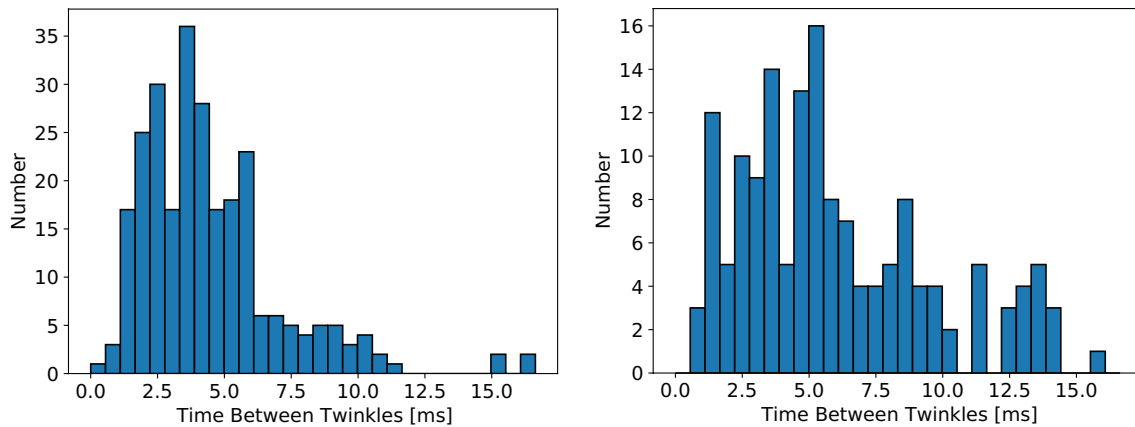


Figure 5. Histogram of the times between subsequent twinkles. Left is 2017, right is 2019 flashes.

only use needle twinkles that occur after the return stroke. Finally, we excluded needles that had a final chi-square fit value greater than 6, which corresponds to 12% of the time between twinkles. In the 2017 flash, we attempted to fit 46 needles. Twenty-one was excluded because they had too few imaged twinkles after the return stroke, and two were excluded because the chi-square fit was greater than 6. We attempted to fit 44 needles from the 2019 flash, 34 of which was excluded due to having too few imaged twinkles. All of the fitted needles from 2019 had a chi-square < 6 .

The results of the fit for both flashes are shown in Figure 7, which shows the factor between subsequent twinkles versus the number of observed twinkles. The error bars are one-standard deviation error bars calculated from the analytical covariance matrix weighted by the resulting chi-square fit value. For the 2017 flash, all the needles from one particular leader are indicated. This is the same leader investigated in further detail in Section 2.5. Figure 7 shows that some needles are consistent with a constant twinkling time (i.e., the twinkle-time factor is within three standard-deviations of 1.0), but there are also many needles that are not consistent with a constant twinkling time. No observed needles twinkle faster over time. The increase in twinkling time can be quite large, even over 30% increase per twinkle. The needles on one leader in the 2017 flash seem statistically consistent with having the same twinkle-time factor, but it is difficult to do a detailed comparison of how nearby twinkles do or do not relate to each other.

Figure 8 shows the distribution of VHF needle lengths and Figure 9 shows the distribution of VHF lengths of individual twinkles divided by the length of the needle, for twinkles with more than one source. The length of each needle is the maximum distance along the fitted axis between any two sources in the needle, and the length of each twinkle is the maximum distance between any two sources in a twinkle. Thus, the

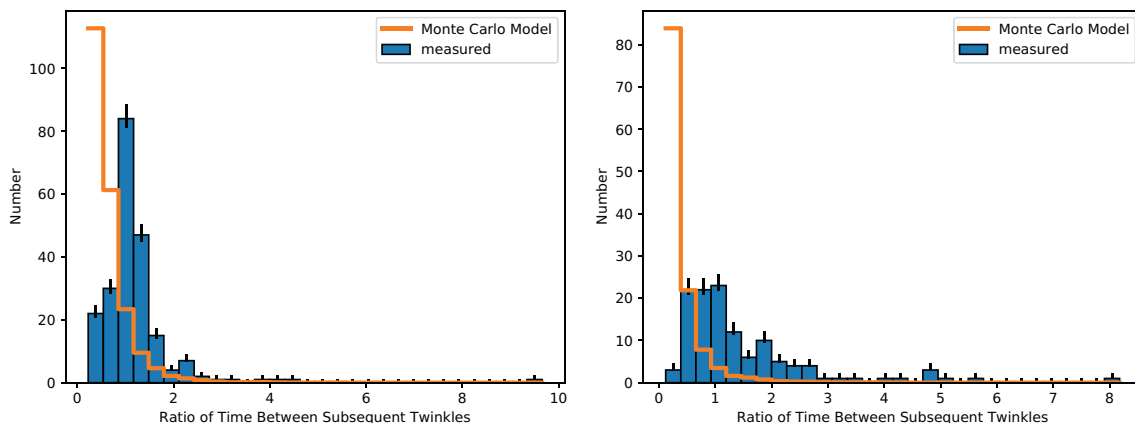


Figure 6. Histogram of the times between subsequent twinkles. Left is 2017, right is 2019 flashes.

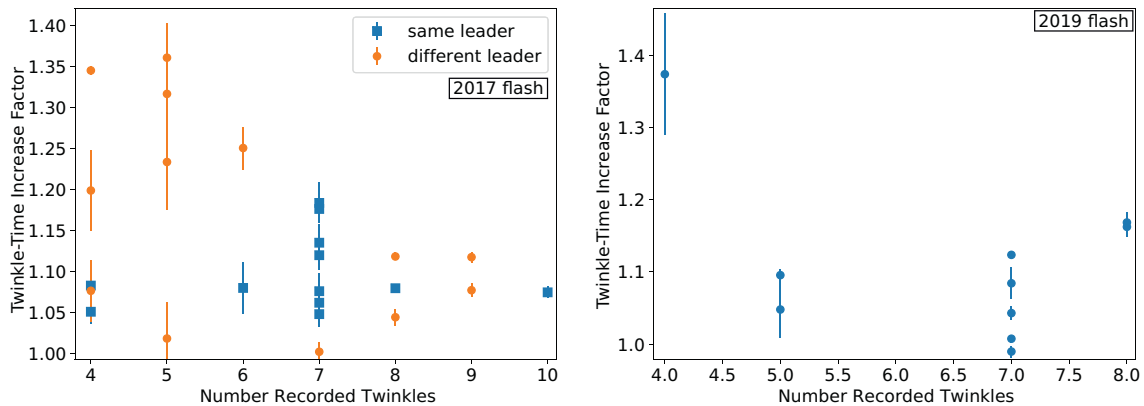


Figure 7. Fitted twinkle-time increase factor, f , from Equation 1, between subsequent twinkling times. Left is 2017, right is 2019 flashes.

VHF twinkle lengths can never be longer than a full VHF needle length. We would like to emphasize that in this study, we can only explore the length over which the twinkles and needles emit in VHF. It is always possible that a twinkle can propagate without emitting VHF, and thus is longer than what our measurements show. Later we will argue that this is probably common.

Figure 8 shows that while some needles can be relatively long (100–200 m), the vast majority are <40-m long with shorter needles occurring more often. Figure 9 shows that twinkles have relatively random VHF lengths relative to the total VHF length of the needle. The distribution of relative twinkle lengths for both flashes is statistically consistent with a uniform distribution (p -values of 0.48 and 0.20, respectively, from a 1-sample Kolmogorov-Smirnov test).

Since, based on the needles shown in Figure 2 and the distributions in Figure 9, it is obvious that each twinkle does not emit mappable VHF over the whole length of the needle, we can explore the distributions of points where twinkles initially and finally emit VHF. Figure 10 shows the location, along the fitted axis, where each twinkle emits VHF closest to the base of the needle, divided by the VHF length of the needle, and Figure 11 shows the VHF location farthest from the base of the needle, divided by the VHF length of the needle, for each twinkle. Figures 10 and 11 show that while twinkles tend to start and stop emitting VHF radiation closer to the base and tip of the needle, respectively, they can start and stop emitting VHF anywhere along the needle.

Since the VHF emission of a twinkle sometimes starts some distance from the main channel, this data could technically imply that some needle twinkles could be bidirectional and have a positive end that propagates toward the main channel. However, this at least cannot be the case for the majority of needle twinkles, since

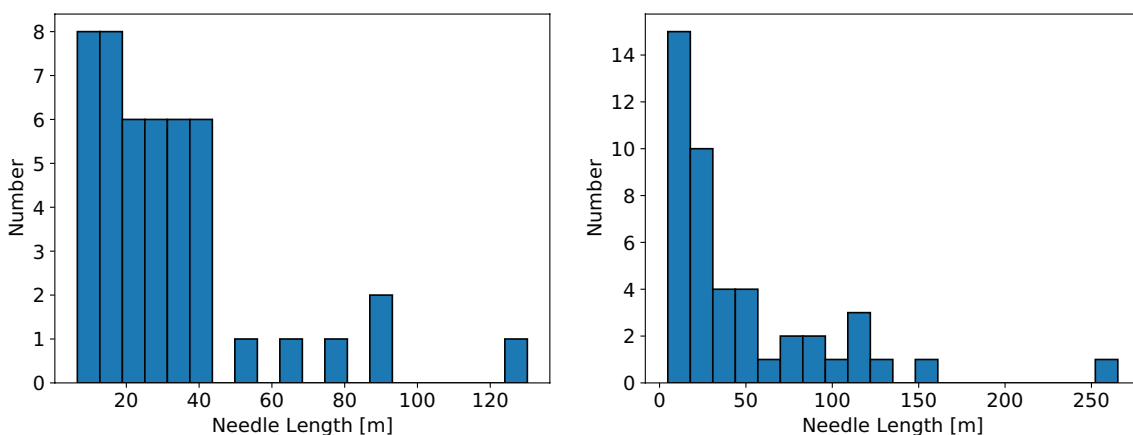


Figure 8. Length of each needle. Left is 2017, right is 2019 flashes.

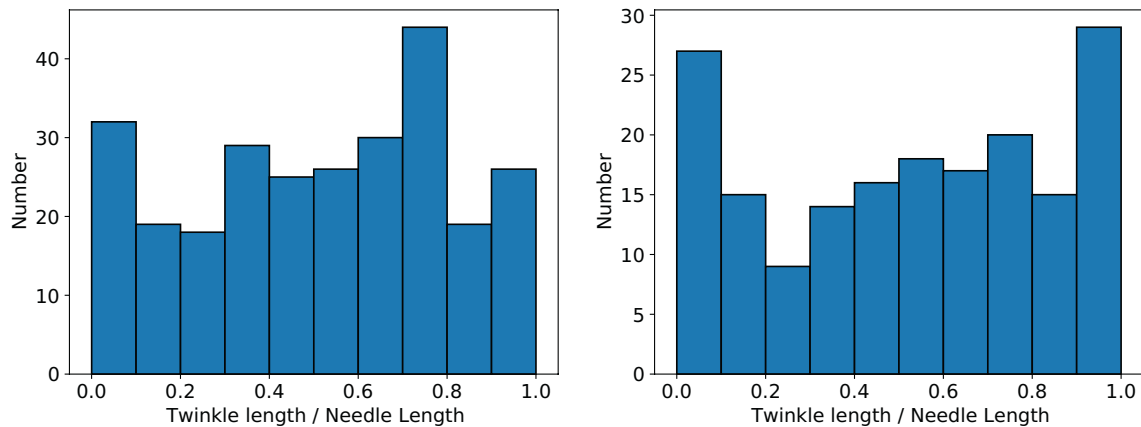


Figure 9. Histogram of length of each twinkle divided by the length of the needle, excluding twinkles of one source. Left is 2017, right is 2019 flashes.

Figure 10 shows that the majority of twinkles emit their first VHF near the positive leader channel. Furthermore, Saba et al. (2020) did not see any optical evidence of a positive end of the needle twinkles. Therefore, the fact that the first located VHF emission of a twinkle is not immediately on the positive leader channel is mostly likely due to a combination of imaging efficiency and twinkles propagating without VHF emission.

In order to show that twinkles, in general, do not extend the VHF length of a needle, Figure 12 shows the difference between subsequent values from Figure 11. That is, positive values in Figure 12 mean that a twinkle ended further along the needle than the previous twinkle, and negative values mean the previous twinkle ended closer to the base. The fact that the distributions in Figure 12, for both years, are centered at zero, supports our observation that twinkles do not tend to extend the VHF length of a needle.

Figure 13 shows the distribution of distances between the VHF source locations and the fitted axis for each needle. Figure 13 essentially shows the VHF width of our needles. This distribution has a peak at 1–2 m from the needle axis, which is consistent with our location accuracy. That is, the needle widths are the same size as, or smaller than, our meter-scale location accuracy.

Figure 14 shows the distribution of twinkle propagation speeds found from the axis fitting discussed in Section 2.1. The distributions in Figure 14 only include twinkles that have more than five sources and the extracted standard error of the fitted speed was <25% of the extracted speed. This distribution shows that twinkles have an extremely wide range of possible speeds. They can propagate as slow as a stepped leader (10^5 m/s), all the way up to the speed of a fast dart leader (10^7 m/s) (Dwyer & Uman, 2014). We have

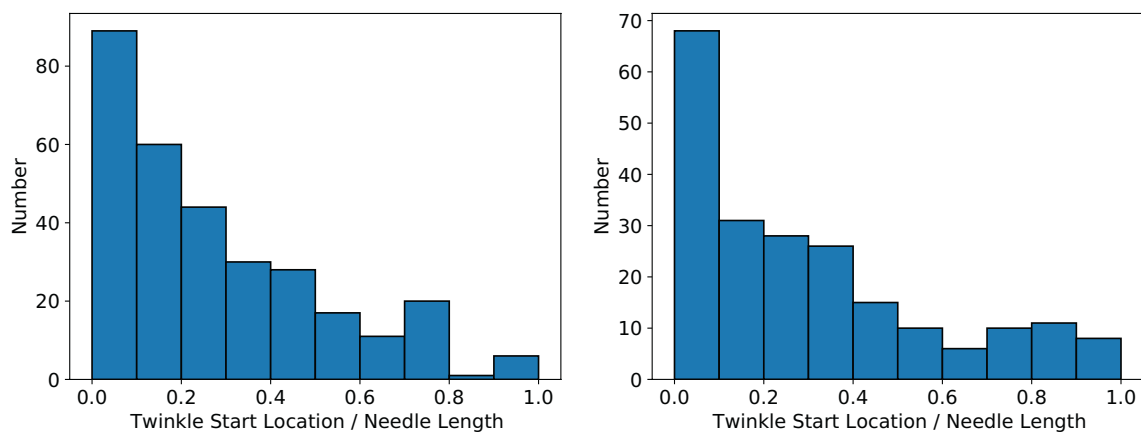


Figure 10. Histogram of the distance between the start of twinkles from the start of the needle, divided by the length of the needle. A “0” means the twinkle started near the beginning of the needle. A “1” means the twinkle started near the end of the needle (thus, the twinkle was necessarily short). Left is 2017, right is 2019 flashes.

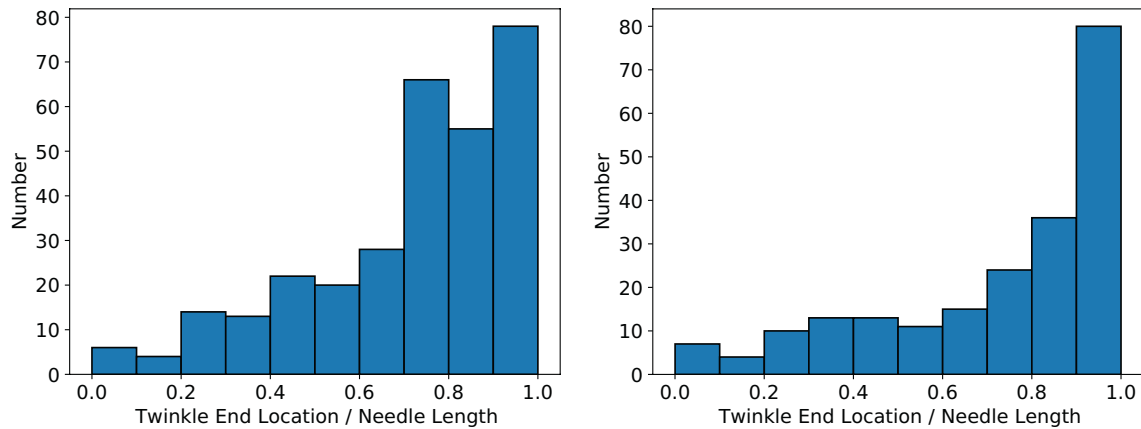


Figure 11. Histogram of the distance between the end of twinkles from the start of the needle, divided by the length of the needle. A “0” means the twinkle was short, and ended at the start of the needle. A “1” means the twinkle ended near the end of the needle (but does not imply the twinkle is long). Left is 2017, right is 2019 flashes.

examined the fits of all twinkle speeds by eye, and while Figure 14 shows the average speed of each twinkle, many twinkles are similar to those shown in Figure 3 in that their propagation will start fast and slow down. Many other twinkles, however, maintain a constant propagation speed. Generating robust statistics for how often a twinkle slows down, however, is difficult and should be explored in future work.

Figure 15 shows the VHF imaged source density versus twinkle propagation speed for each twinkle that we could calculate a speed for. The source density was simply the number of imaged sources in the twinkle divided by the VHF twinkle length. The 2017 flash has a very strong correlation between density and speed. The slower twinkles tended to have more sources per meter. The 2019 flash is similar, but the trend seems to be weaker. It is not clear if faster twinkles emit more VHF radiation, and so overwhelm the imager, or emit less VHF radiation.

A close inspection of Figure 2 shows that the VHF sources inside of each twinkle tend to cluster in time. This is emphasized in Figure 16, which shows the distribution of time between VHF sources inside of individual twinkles. If the VHF sources were scattered randomly in time then this distribution should be exponential, but instead we see a strong increase over an exponential at small time differences. This is extremely similar to the VHF bursts we discussed in Hare et al. (2020), which we found along negative leaders, where we attributed the large peak at small time separation ($<0.5 \mu\text{s}$ in Figure 16) to stepping. This implies that needles, at least sometimes, tend to step-like negative leaders.

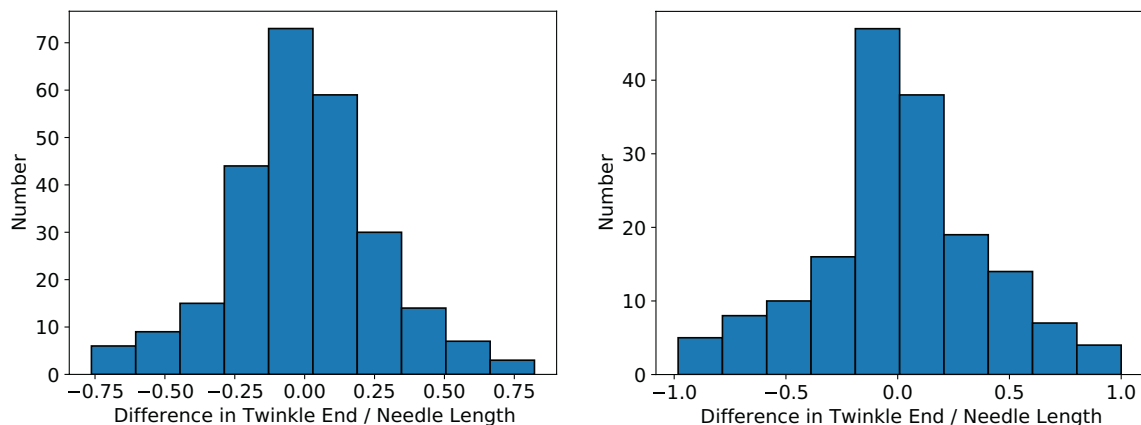


Figure 12. Histogram of the distance between the ends of subsequent twinkles, divided by the length of the needle. This is the difference between subsequent values from Figure 11. Left is 2017, right is 2019 flashes.

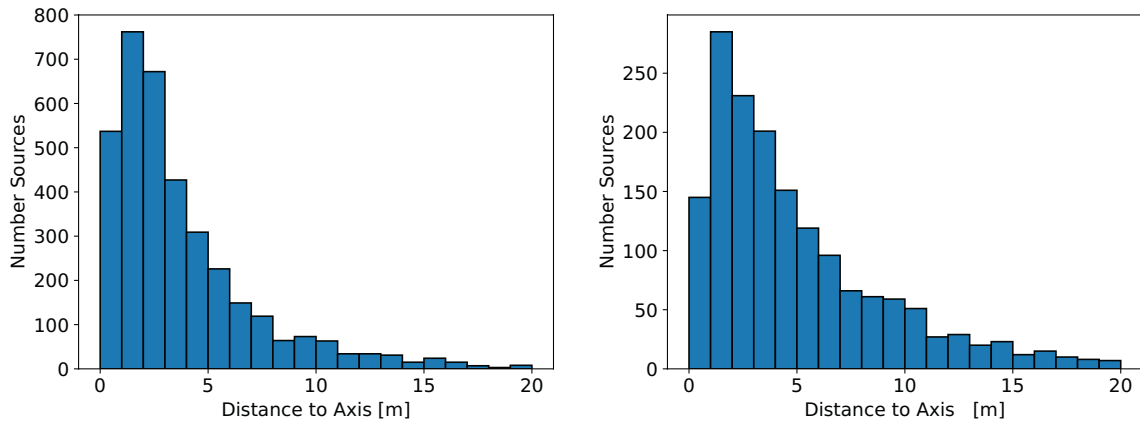


Figure 13. Distance from VHF sources in needles to the fitted axis. Left is 2017, right is 2019 flashes.

Figure 17 shows the distributions of uncalibrated VHF pulse amplitudes from needles and negative leaders during the 2017 flash. These distributions were simply calculated by taking the amplitude of the associated VHF pulse on a reference antenna, squaring it and multiplying by distance to source squared. Similar to previous work, Figure 17 clearly shows that needles emit lower VHF power than negative leaders on average (Li et al., 2020; Shao & Krehbiel, 1996). However, unlike previous work, we have successfully separated needles and recoil leaders, and the distributions shown in Figure 17 contain, at most, very few sources from recoil leaders. Figure 17 also appears to show that high-amplitude tail of VHF amplitude distributions has different shapes for negative and positive leaders, however, such subtleties need to be interpreted extremely carefully as Figure 17 does not account for amplitude-dependent imaging efficiency.

2.3. Negative Stepped Leaders and Needles

Figure 18 shows a time slice of the 2017 and 2019 flashes, where in both flashes, all negative leaders cease propagating (at $T = 72$ ms and $T = 115$ ms for the 2017 and 2019 flashes, respectively) and there is a period of 25–30 ms where there is no negative leader activity, then a new negative leader starts (at $T = 100$ ms and $T = 137$ ms in the 2017 and 2019 flashes, respectively), as indicated in the figure. Figure 18 shows that during both flashes, when a new negative leader starts the needle activity is suppressed. However, this relationship is complex, as Figure 18 also clearly shows that needle activity seemed to increase as the negative leader in the 2017 flash approached ground, between times $t = 60$ ms and $t = 70$ ms. This is a common feature we see in all imaged flashes, but we cannot exclude that possibility that it is at least partially due to the stronger VHF emissions from negative leaders masking the VHF emission from needles.

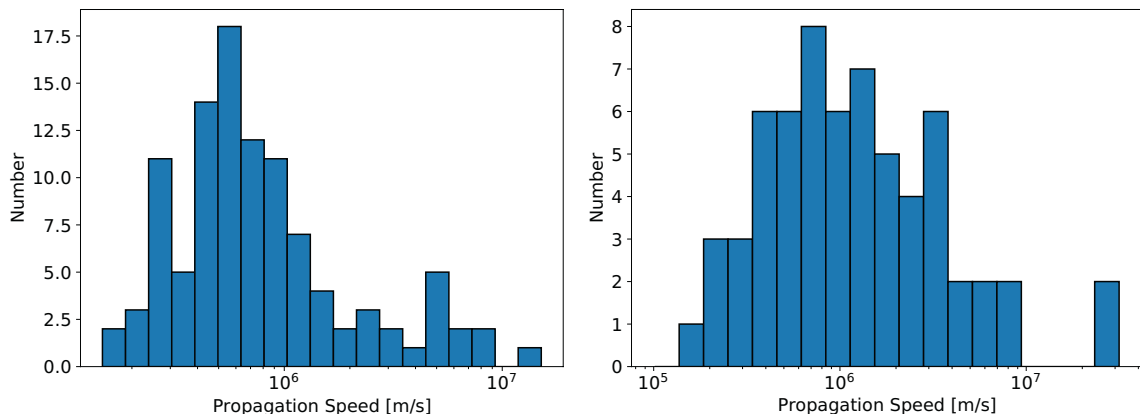


Figure 14. Speed of the twinkles. Left is 2017, right is 2019 flashes.

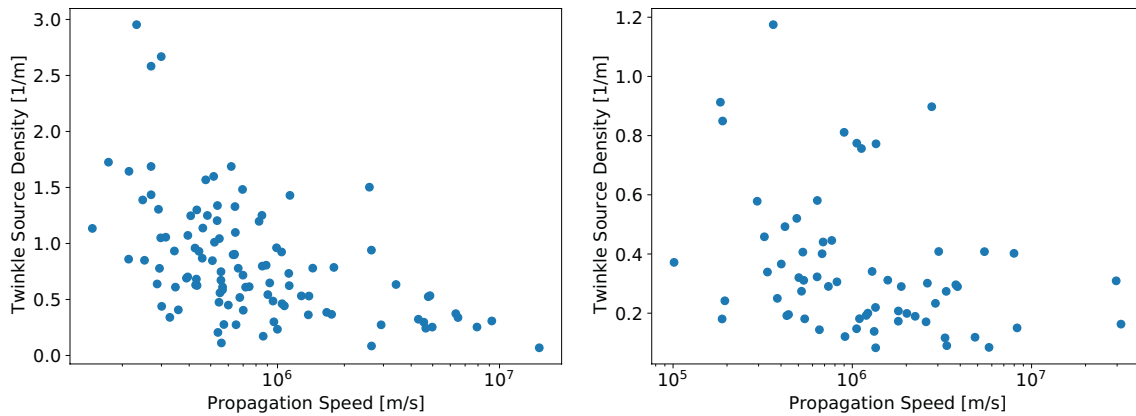


Figure 15. VHF source density per twinkle versus the speed of the twinkle. Left is 2017, right is 2019 flashes.

This suppression of needles, however, is not unique to negative leaders. The return stroke at $T = 72$ ms in Figure 18 during the 2017 flash seems to result in a large “hole” in needle activity following the return stroke. This lack of needles immediately after the return stroke is not an imaging artifact, as we do not observe any VHF pulses from lightning above noise for about 1 ms after the return stroke. We have imaged one other flash with a return stroke, and it is ambiguous if that return stroke quenches needle activity or not. Further work is needed to explore the precise behavior of return strokes as imaged by LOFAR.

2.4. Recoil Leaders and Needles

The interactions between recoil leaders and needles are complex and varied. Here, we report some of our observations on a few of the interactions we have observed. First, on rare occasion, we observe that a recoil leader will sometimes initiate a needle twinkle as it passes by the needle. One example is given in the appendix of Hare et al. (2019) shows the clearest example we have observed. The few other cases of recoil leaders inducing needle twinkles have not been nearly as clear.

We also regularly observe recoil leaders occurring at the same time that needles stop twinkling. Figure 19 shows a section of time during both flashes when there is significant recoil activity and very little negative leader propagation. The recoil leaders are clear in the altitude versus time panel as vertical bars and the needles appear as horizontal bands. This figure shows in both flashes a tendency of needles to build-up in intensity and then quench at the same time as a recoil leader, two examples are at $T = 198$ ms in the 2017 flash and $t = 360$ ms in the 2019 flash.

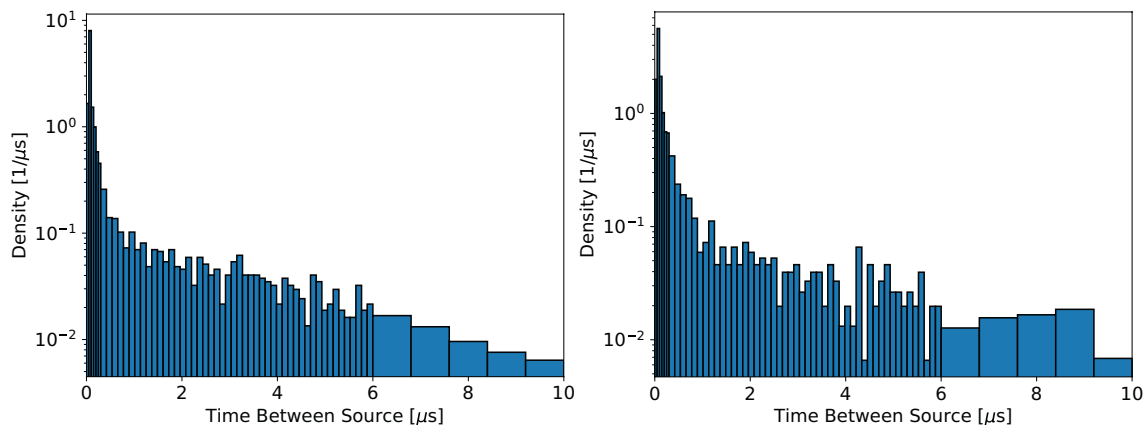


Figure 16. Distribution of time between sources in twinkles. Left is 2017, right is 2019 flashes.

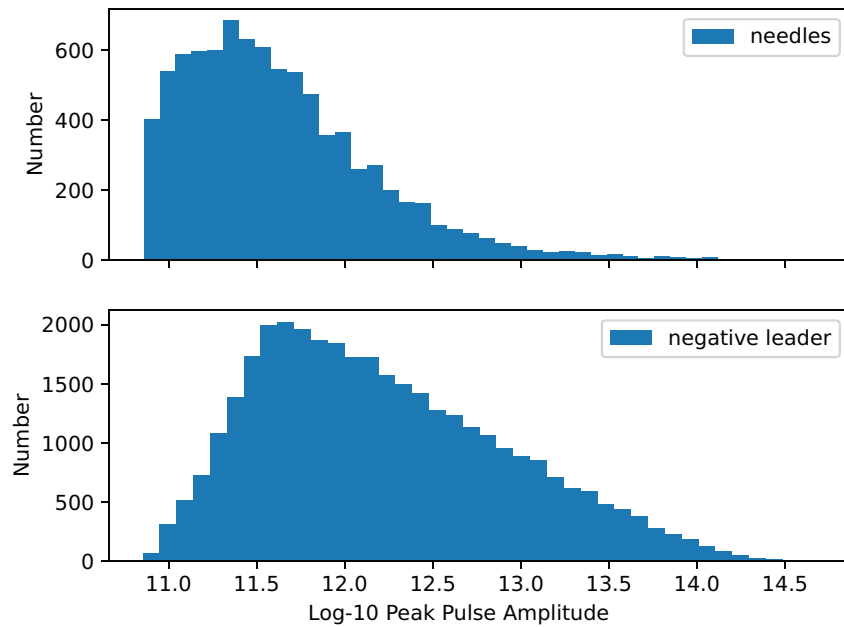


Figure 17. Distribution of VHF power emitted by needles and negative leaders during the 2017 flash.

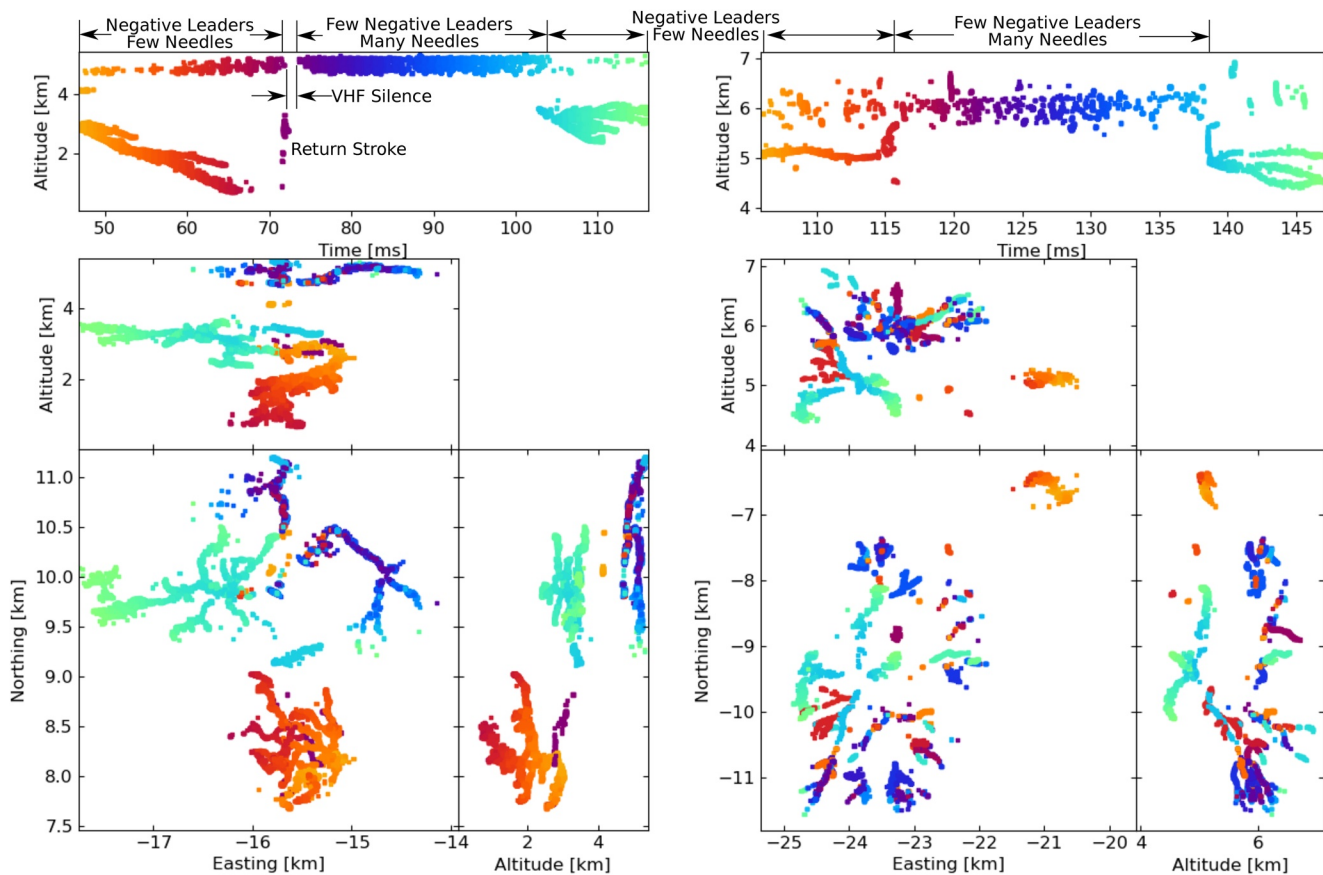


Figure 18. Relative relationship between negative leader and needle activity. Periods of negative leader activity and low needle activity, and vice versa, is indicated. The return stroke and following period of VHF silence are also indicated for the 2017 flash. Left is 2017, right is 2019 flashes.

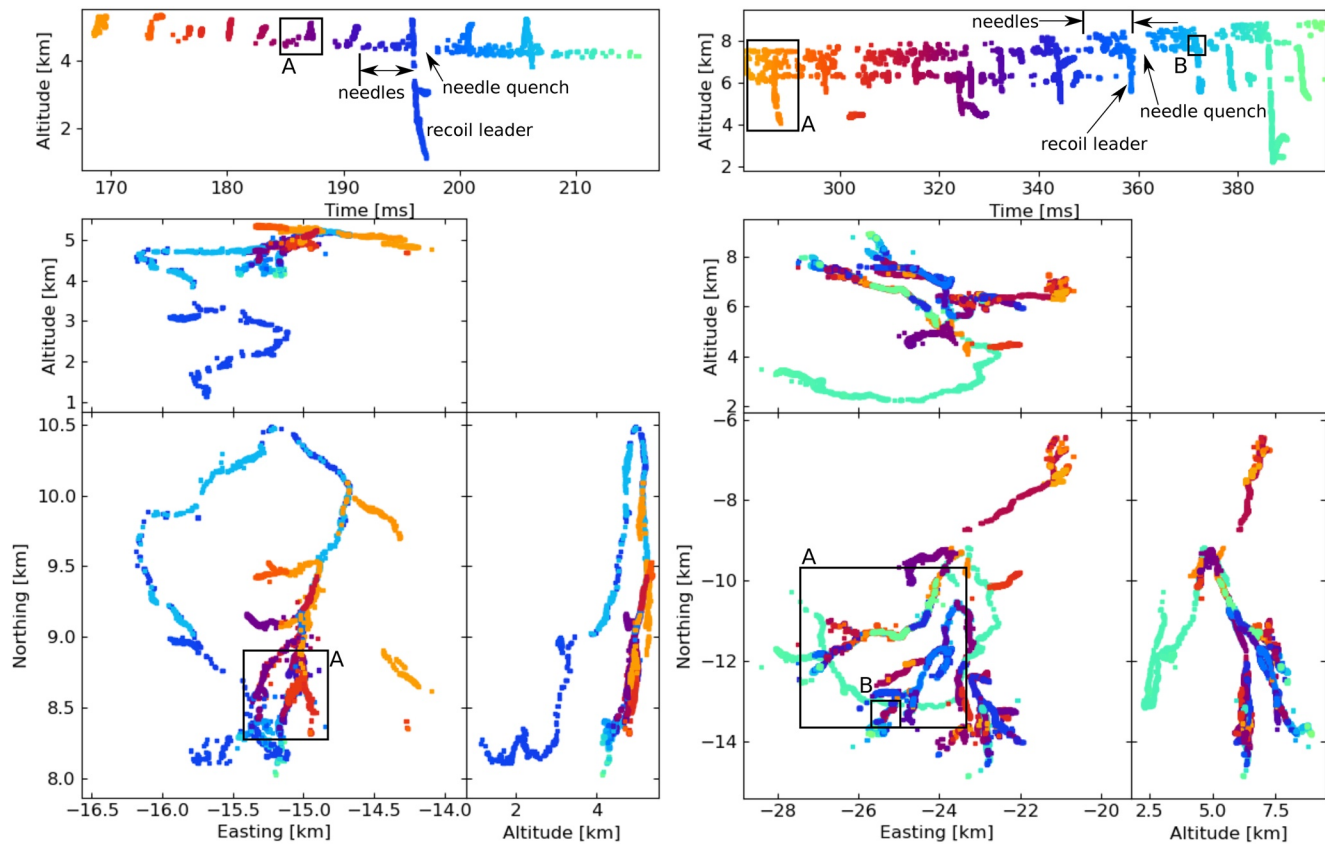


Figure 19. Relative relationship between recoil leader and needle activity. One group of needles, recoil leader, and period of needle silence is indicated for each flash. Rectangles labeled “A” for both flashes indicate the region focused-on in Figure 20. The rectangles labeled “B” in the 2019 flash show the region focused-on in Figure 21. Left is 2017, right is 2019 flashes.

Figure 20 shows a zoom-in on a recoil leader from 2017 to 2019 that both occur at the same time that needle activity quenches. In both of these cases, and in many others, we see that the recoil leader starts farther up the leader branch (closer to the initiation-point of the flash) than the active needles, and the needles cease all activity for some time after the recoil leader. Needles on other leader branches, such as in the shown 2019 case, do not seem to be affected.

Of course, there are always variations from the standard scenario. Figure 21 shows an unusual case from 2019. This same recoil leader is shown in Figure 19 at $T = 371$ ms, in which this recoil leader appears similar to the others in that it occurs at the same time as a quenching of needle activity. However, a zoom-in to the beginning of the recoil leader, as in Figure 21, shows that there was some kind of positive breakdown (shown in red) $400 \mu\text{s}$ before the recoil leader. This positive breakdown reached 1×10^7 m/s in speed and occurred along a stretch of already-extended channel. This positive breakdown leads to an increase in needle activity over the channel that it propagated, and was then followed by a normal recoil leader, after which there was no needle activity on this branch for 4 ms.

2.5. Needle Structure Along the Positive Leader

Top panel of Figure 22 shows the distance of VHF sources along a positive leader channel of the 2017 flash versus their time. It was constructed by manually placing a linear spline over the path of the positive leader, choosing branches that propagated the furthest. Each source within a distance of 125 m from that spline is shown in the top panel of Figure 22, at the time of occurrence and at the distance measured along the spline. The line in the top panel of Figure 22 shows the location of the VHF source that is furthest along this leader branch. The bottom panel of Figure 22 shows the histogram of all located sources (not just those along this branch), in order to compare the temporal density of needles to the temporal density of all located

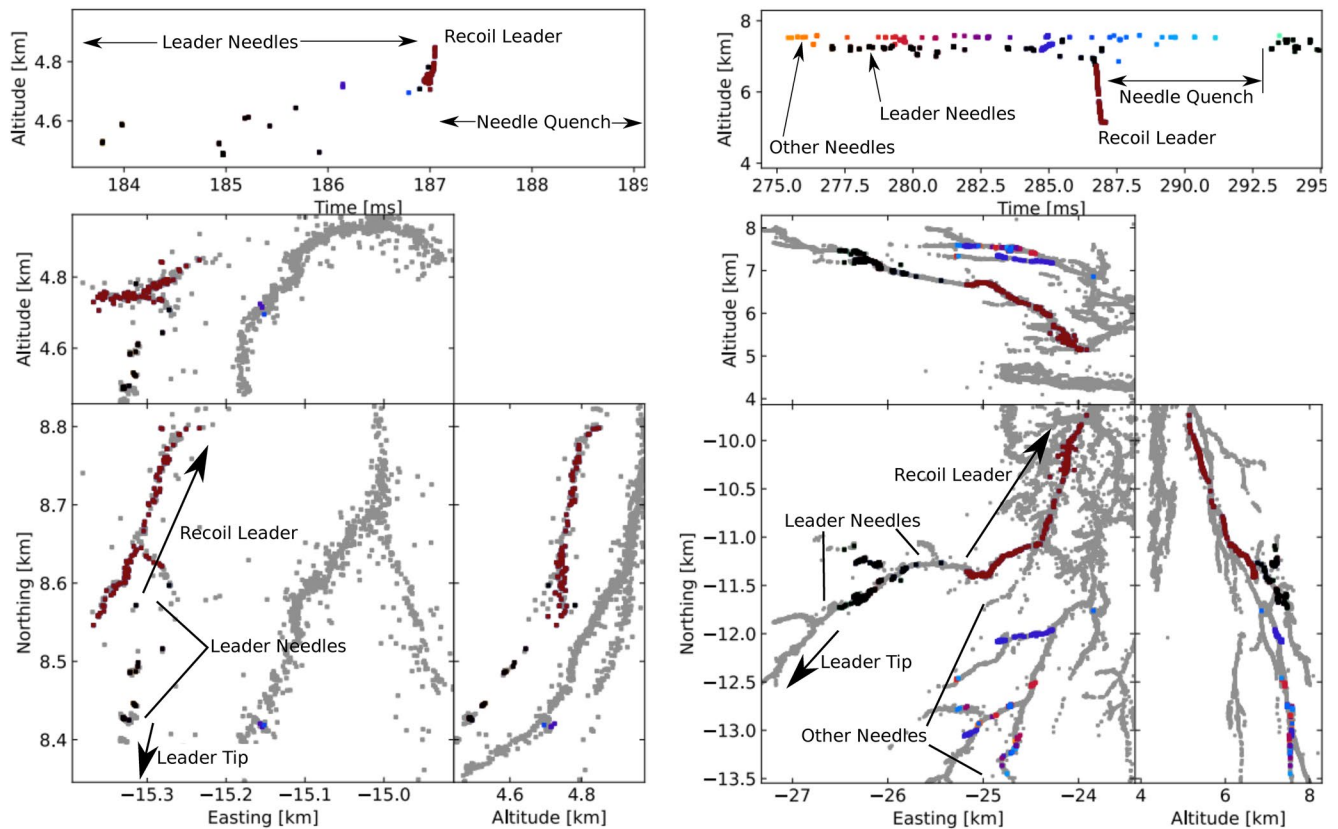


Figure 20. Two examples of a recoil leader occurring at the same time as a cessation of needle activity, as indicated by the rectangles labeled “A” in Figure 19. Gray dots show all located VHF sources. The dark red-brown dots show VHF sources from a recoil leader. Black dots show needle activity on the same leader branch as the recoil leader, and needle activity from other leaders are colored by time. The recoil leader and its direction, needles on the same leader (and different leader for 2019 flash), time period of needle quench, and general direction of leader tip is indicated. Left is 2017, right is 2019 flashes.

VHF sources. We choose a section of time before any significant recoil activity during the 2017 flash. We did not make a similar plot for the 2019 flash due to amount of recoil activity. A similar figure was shown in Pu and Cummer (2019).

Figure 22 shows that the density of needle activity over the leader is very nonuniform. As discussed previously, the observed needle activity is strongly anticorrelated with negative leader activity. For example, the imaged needle activity is highest 5–30 ms after the return stroke, which is when there are fewest total VHF sources as there were no propagating negative leaders between the return stroke and $T = 110$ ms.

Similar to the findings of Pu and Cummer (2019), the solid line in Figure 22 shows that there is a point on the positive leader that has copious needle activity behind it and no activity in front. This propagates forward at about 5×10^4 m/s (Pu and Cummer (2019) measured 1×10^5 m/s and Saba et al. (2020) measured about 4×10^4 m/s, both projected in 2D), and we refer to it as the needle production head. It is important to note that this head is not necessarily the location of the positive leader tip, as we cannot image the location of the positive leader tip in VHF. There are two ways we could infer a rough guess as to the distance between the needle production head and the leader tip. First, is that the needle production head moves forward in jumps due to the discrete nature of needle activity (as shown by the solid line in Figure 22). If the positive leader propagates smoothly, then its location in Figure 22 would be represented by a smooth line. In this case, the distance between the needle production head and the positive leader tip cannot be much smaller than the jumps in the needle production head. That is, it is very difficult to draw a smooth line (representing the positive leader tip location) in Figure 22 such that the distance between that line and the needle production head is significantly smaller than the forward-jumps in the needle production head. Figure 22 shows that these jumps are about 250-m long, and thus the distance between the needle production head and leader tip is most likely larger than 250 m. Second, at the beginning of the flash, there is a period of about 15 ms

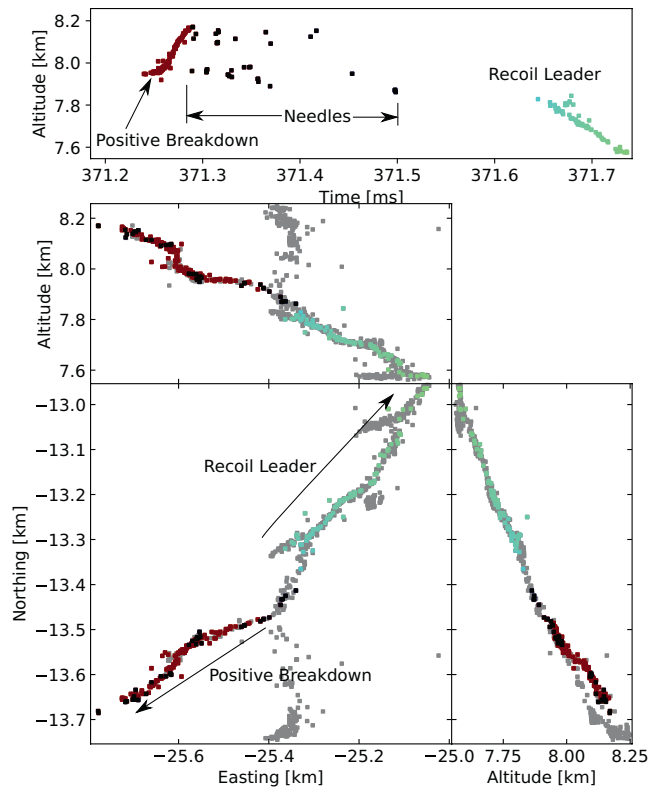


Figure 21. An example of an unusual event from the 2019 flash. The dark red-brown dots show some kind of positive breakdown. Black dots show needle activity, and teal-blue dots show a recoil leader, also indicated by labels.

between when we first observe the initial downward negative leader and the first needle activity. If we assume that the positive leader propagated during this time between 5×10^4 and 10×10^4 m/s, then the tip of the positive leader could be around 700–1,500 m in front of the needle production head. Saba et al. (2020) found that the tip of the positive leader was around 100–200 m in front of the needle activity for the upward positive leaders they observed. In contradiction with Pu and Cummer (2019), we find that needle activity occurs over a very long distance behind the needle front, with little to no decay in activity over distance. During the first 75 ms of the flash, the needle activity seems very continuous over the entire leader. After 80 ms, the needles seem to twinkle over a 2.5–3.0-km length of channel.

Note that although there is a period of time with no needle activity after the return stroke, when the needle activity starts up again the needle production head moved forward by about 250 m, consistent with continuous silent propagation after the return stroke. Assuming that the tip of the positive leader maintains a relatively constant distance in front of the needle production head, this implies that the positive leader continued to propagate after the return stroke during the silent period of no received VHF signal.

Figure 23 is very similar to Figure 22, but only shows the needles in this region that were used in finding our statistical distributions discussed in previous sections. Figure 23 emphasizes the relationship between needles that are spatially close. Particularly, that twinkles of nearby needles are not correlated or anticorrelated. That is, we observe that twinkles that are spatially relatively close can twinkle at difference rates. A good example of this is two needles that are directly next to each other, shown in Figure 23 at a distance of about 0.5 km along the leader, after $T = 50$ ms. These two needles seem to twinkle independently at different rates. This observation is precisely opposite to that made by Saba et al. (2020). Saba

et al. (2020) seemed to observe that nearby needles twinkle out-of-phase with each other, which lead Saba et al. (2020) to hypothesize that needle twinkles could be due to some kind of wave that propagates down the channel. We believe that Saba et al. (2020) seemed to observe this behavior because they only focused on a relatively small section of channel. If the needles twinkle at a regular rate, and the distance between needles is about equal to the speed of the leader times half the time between twinkles (which is the case in their data), then the twinkles from nearby needles will naturally appear to occur out-of-phase even if the needles have no interaction at all. Close examination of Figure 3 in Saba et al. (2020) shows support not only for downward-going waves, but also equal evidence for upward-going waves, which strongly implies that downward-going twinkle-inducing waves are an observational artifact.

3. Discussion

3.1. Comparison to Bidirectional Leaders

In addition to needles, previous work has also observed in both VHF and optical that bidirectional leaders can initiate behind positive leader tips, where the negative end will propagate and connect to the main positive leader (Pu & Cummer, 2019; Warner et al., 2016; Yuan et al., 2019). At first glance, it seems that bidirectional leaders and needles may possibly be the same phenomena. However, there are three main reasons why these two phenomena are clearly different. The first reason is scale. Bidirectional leaders initiate about 200–500 m from the positive leader channel (Pu & Cummer, 2019; Yuan et al., 2019), and thus are significantly longer than needles which are rarely longer than 100 m. The second reason is polarity. The negative end of bidirectional leaders propagates toward the positive leader branch, whereas the negative end of needles propagates away from the positive leader. In addition, the positive end of bidirectional leaders is at least sometimes visible in VHF due to needle activity (Pu & Cummer, 2019), whereas needles show no evidence

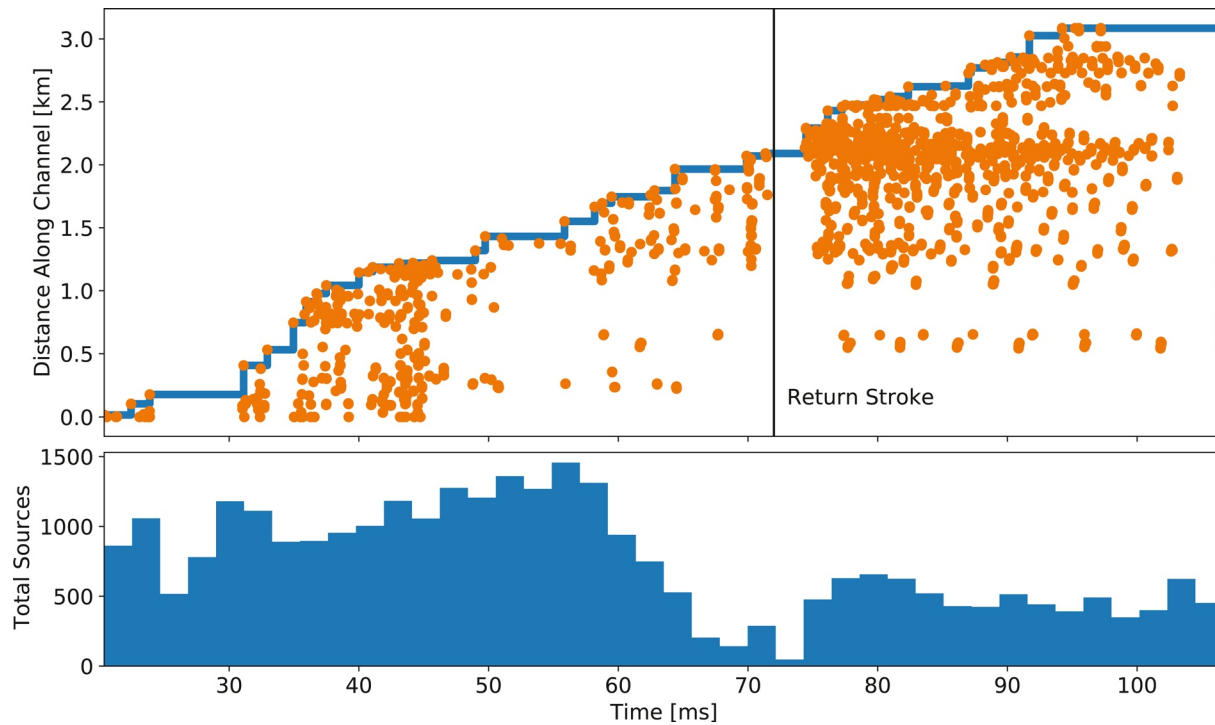


Figure 22. Top panel shows location versus time of VHF sources along a positive leader channel of the 2017 flash. Colored line shows the distance of the source that is farthest along the positive channel. A vertical black bar shows the time of the return stroke. Lower panel shows histogram of all located sources (not just those on this leader).

(either in VHF or optical) of a positive end. Finally, needles twinkle at a very regular rate in both VHF and optical, whereas bidirectional leaders do not show any similar kind of activity.

3.2. Field Reversal Mechanism

The fact that needles twinkle at a fairly regular rate that can decrease over time, neighboring needles can twinkle at different rates, each twinkle is a form of negative propagation, and that the twinkles propagate away from the positive leader, makes them difficult to explain. Hare et al. (2019) postulated that there must

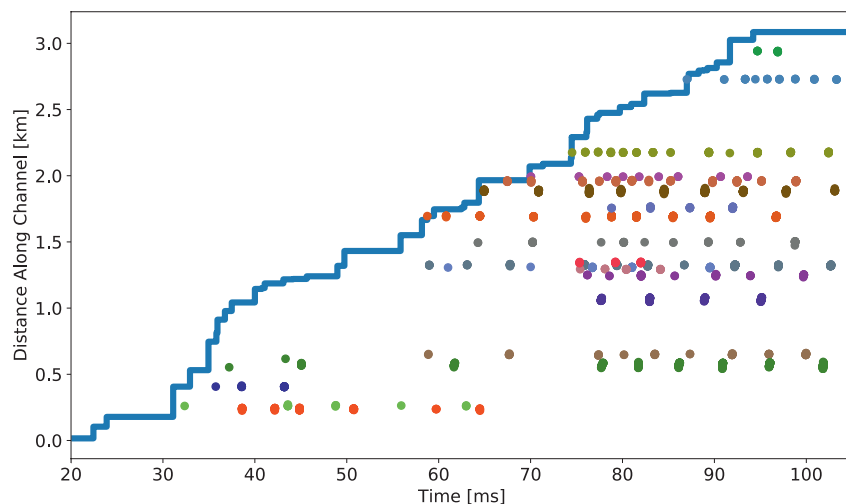


Figure 23. Location versus time of VHF sources from selected needles along a positive leader channel of the 2017 flash. Colored line shows the distance of the source that is farthest along the positive channel.

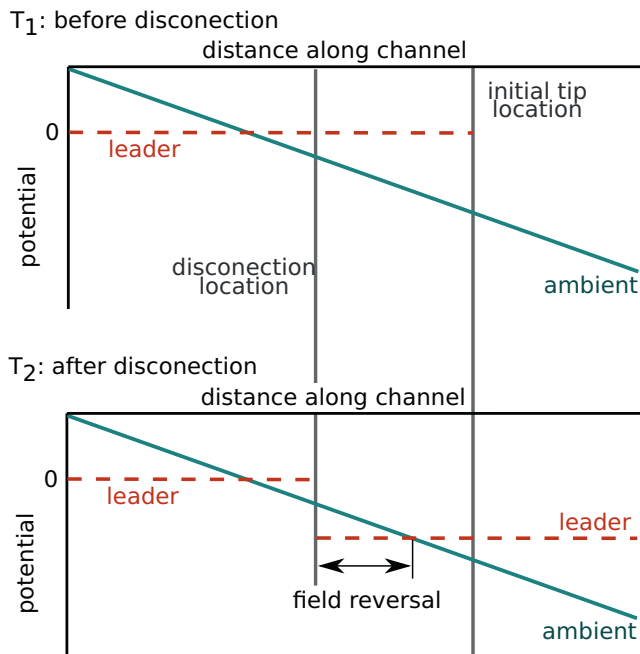


Figure 24. Most basic effects of leader disconnection. The ambient electric potential and leader potential are shown versus distance along the leader, before and after an insulating disconnection forms in the leader. A step-like discontinuity in the potential along the leader is shown due to the disconnection.

be an electric field reversal along the positive leader; where the tip of the positive leader has an outward-pointing electric field (as one would expect), but the electric field along the body of the positive leader points inward. Hare et al. (2019) further hypothesized that one possibility for field reversal is if the positive leader became disconnected from the negative leader so that the positive leader would gain a more and more negative potential over time as it propagated, and needle twinkles would occur in order to equalize the potential between the leader and the ambient field around it. In this section, we will thoroughly discuss the possibilities for how the electric field perpendicular to the leader channel could flip direction and point toward the channel. We will start with the simplest possible scenarios and gradually make the picture more realistic.

3.2.1. Channel Disconnection Without and With Finite Resistance

The first scenario we consider is the simplest case of a channel disconnection. That is, the leader channel is perfectly conducting and all the charge of the leader lies directly on the conducting leader (we ignore corona-sheath effects for the moment), and a perfectly insulating disconnection develops on the positive leader. In this scenario, diagrammed in Figure 24, as the positive leader propagates in a uniform ambient electric field its electric potential will become more negative over time (since the electric field at the tip is roughly constant). Eventually, the later section of the positive leader (as shown in Figure 24) will gain a more negative potential than the ambient field. This will cause the electric field perpendicular to the later-half of the leader to point toward the channel, possibly inducing needle activity. Note that since we are only considering surface charge directly on the conducting leader, only the potential difference

between the leader and the ambient field is important. Since each needle twinkle neutralizes the electric field in its immediate vicinity, the amount of needle activity will be proportional to the rate of change of the leaders potential, and thus be uniform all along a section of leader that will grow in length at the same speed that the leader propagates. This prediction is very similar to what we observe in Figure 22. This picture predicts a possibly large distance between the needle production head and the tip of the positive leader. As discussed in Section 2.5, our data support the possibility that there is about 750–1,500 m between the needle production head and leader tip, whereas Saba et al. (2020) observed there was only about 100–200 m between the leader tip and first needle activity.

Next, we consider the effect of resistance on the disconnection hypothesis. If the channel is not perfectly conducting and the break is not perfectly insulating then two changes from the basic picture will emerge.

- (1) The change in leader potential will not be a sharp discontinuity (as represented in Figure 24), but will occur more smoothly in space.
- (2) Current will flow over the disconnection, thus the field reversal will occur more slowly. The magnitude of the current will depend on the difference in potential across the leader (depending on how ohmic the leader channel is). In an extreme scenario, it is possible that the current across the disconnection could eventually equal the current injected into the positive leader by the propagating tip, in which case the potential will stabilize and shut down all needle activity on this leader. However, since the relationship between current and potential in a leader is not understood, it is not clear how quickly this effect will occur or if it will occur at all. It is even possible that needle twinkling slowing down over time is a result of this saturating field reversal effect.

At first glance, this disconnection hypothesis seems to have two difficulties.

- (1) First, needles have been observed on leaders that seem to be well-conducting. Saba et al. (2020) observed needles on upward propagating leaders, and in this study, we observe needle activity just before a return stroke that quenches the needle activity but does not show any VHF emission along the positive

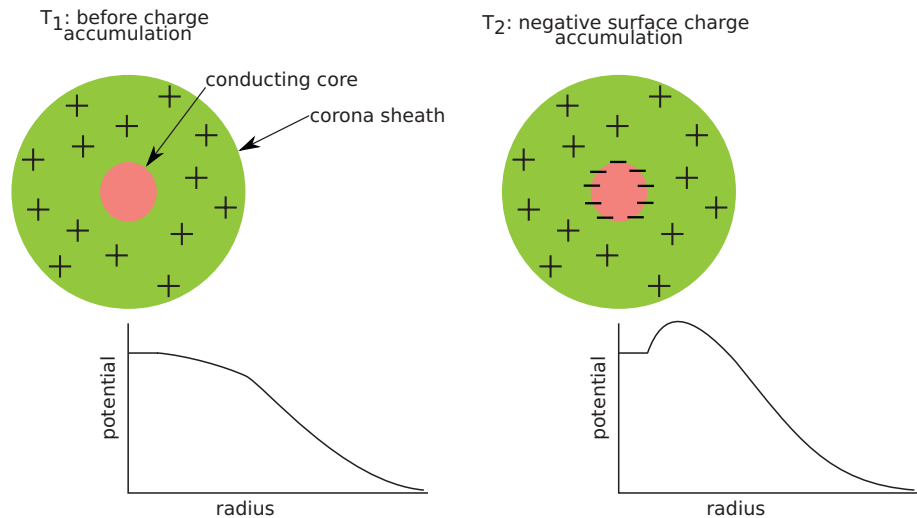


Figure 25. The corona-sheath effect. Top portion shows the conducting core and corona sheath of the leader, and the positive charge density locked in the corona sheath. The bottom portion shows electric potential versus radius. The right side shows the difference if the total charge at this location becomes more negative, in which case negative charge could accumulate on the conducting leader and induce a more complex electric potential versus radius.

leader (thus implying that just before the return stroke there was some conducting connection between positive and negative leaders while the needles were active). Similarly, both Pu and Cummer (2019) and Saba et al. (2020) explicitly state they see no evidence of a disconnection. This lack of evidence of a disconnection, however, should be not surprising as it is not at all clear how channel resistance can be measured through high-speed camera or VHF observations. Furthermore, we have discussed that the disconnection hypothesis is still applicable when the positive leader channel carries current but is highly resistive, which could have been the case in Saba et al. (2020) and before the return stroke observed in this study.

- (2) Second, Pu and Cummer (2019) argues that the disconnection hypothesis predicts that needle activity should primarily occur around the disconnection which is contradictory with the observation of a needle-production front. As discussed above, this is not correct. The disconnection hypothesis predicts needle activity over long lengths of positive leader channel where the channel has more negative potential than the ambient field, not just near the disconnection.

The disconnection hypothesis does precisely describe the interactions we observe between recoil leaders and needles as discussed in Section 2.4, where we observe needle activity increases until a recoil leader occurs and quenches the needle activity because it equalizes the potential across the section. It seems that the recoil leaders quench needle activity because they reconnect the positive and negative leaders of the flash. After the recoil, the channel cools down until a portion of channel becomes highly resistive again, causing the needles to start twinkling again. Needle activity increases as the channel becomes more resistive until another recoil leader occurs, resulting in a cycle that was predicted by Hare et al. (2019). Hare et al. (2019) also speculated that needles play an active role in this cycle, essentially creating positive feedback. More work is needed to show if this positive feedback actually occurs.

3.2.2. Corona-Sheath Effect

Next, we consider a more realistic situation with corona sheath charge. In this case, it is possible for a field reversal to occur when the leader still has a more-positive potential than the ambient field. This corona-sheath effect, as roughly detailed in Figure 25, occurs when the leader charge density (charge on conductor plus charge in corona) at one spot leader becomes more negative over time. Note that it is not necessary for the leader charge density to become negative in absolute terms. The result is that negative charge will accumulate on the surface of the conductor, inside of the still positive insulating corona sheath, producing an electric field that points toward the leader inside the corona sheath and possibly outwards outside the corona sheath. This corona-sheath effect could become important in two different situations.

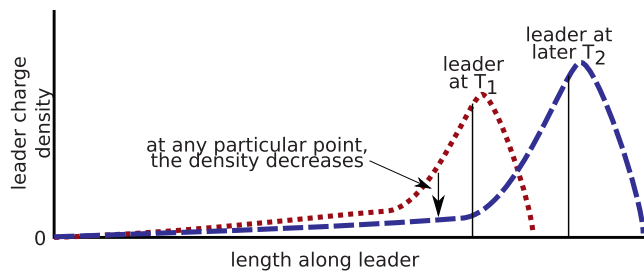


Figure 26. Propagation-induced field reversal. While the total charge of a leader increases as it propagates, the total charge density at any one spot must decrease, possibly leading to the corona-sheath affect.

(1) A leader at a uniform potential does not have a uniform charge density. That is, most of the charge is concentrated near the tip of the leader. Therefore, as illustrated in Figure 26, a point on the positive leader starts its life at the tip of the positive leader with a large total charge density. But, as the leader propagates, the total charge density at them same point must decrease in order for the leader to maintain a constant potential. Via the corona-sheath effect this could result in an electric field reversal just behind the tip of the leader. We refer to this as propagation-induced field reversal. However, it is not clear how this mechanism could produce the observed repeated twinkling, as we would expect the first needle twinkle to discharge the corona sheath. Furthermore, this effect probably decays nearly exponentially behind the tip and so probably could not produce needle activity over 3 km of channel.

(2) The corona-sheath effect will also enhance the field reversal due to a disconnection. Pu and Cummer (2019) predicted that this enhancement should occur mostly near the disconnection, as the negative charge density on the channel is highest near the disconnection. However, this is not correct. As discussed above, if the leader is well-conducting (except for the disconnection), then the field reversal due to a disconnection will be mostly constant along a long section of leader. Since the enhancement due to the corona sheath is proportional to the charge density in the corona, it will also be uniform along the positive leader (to the extent that the corona charge density is uniform). However, as illustrated in Figure 26, the leader charge density far from the tip is probably quite small. Thus, it is entirely likely that the corona sheath near the disconnection could have already been discharged (possibly via needle activity), negating this effect.

In Section 2.5, we observed that nearby needles can twinkle at different rates. Neither the disconnection hypothesis nor propagation-induced field reversal can explain this observation. It is possible that needles can alter the capacitance of the lightning channel, such that different needles require a different amount of charge before the perpendicular electric field is strong enough to initiate a twinkle.

3.2.3. Channel Current Pulses

It is entirely possible that current pulses propagating along the positive leader channel (such as recoil leaders) could deposit negative charge in a needle and cause it to twinkle (Maslowski & Rakov, 2009). One example of this was even shown in Hare et al. (2019, Supplementary Material). However, apart from this one example, we have not found any other times where this conclusively occurs. In addition, Saba et al. (2020) found no correlation between recoil leaders and needle activity. It is possible that the needle twinkles we observe could be due to imaged current pulses, but our data show that this is not the case for the majority of needles. Figures 6 and 7 show that needle twinkles occur at a very regular rate that slows down over time. This would mean such current pulses would also have to occur at a very regular rate that decreases over time, which seems very unlikely. Furthermore, this would predict that needle twinkling on one channel should show correlations between needles. Figures 22 and 23 show that not only do we not observe any correlation between needle activity on one channel, but also that nearby needles can twinkle completely independently from each other. Thus, our data show that while recoil leaders and similar phenomena can sometimes induce needle twinkling it must be very rare.

3.3. Twinkle Propagation

One obvious question is, what is the nature of twinkle propagation? Do twinkles produce highly conducting channels, like leaders, or not? Saba et al. (2020) clearly shows that needle twinkles have strong light emission; however, this does not necessarily imply high conductivity (Malagón-Romero & Luque, 2019). In this study, we have presented significant data pertaining to the nature of the propagation of twinkles. First, we have observed that needle twinkles have an extremely wide range of propagation speeds. Everywhere from 10^5 m/s up to and over 10^7 m/s, as shown in Figure 14. The initial observation by Hare et al. (2019)

missed this wide variety of speeds, probably because the fastest needles are more rare and they tend to have very few VHF sources. Figure 2 is a perfect example, as the 2017 twinkle at $T = 56$ ms propagated at 1.5×10^7 m/s, but only had VHF sources at the base and tip of the needle and was not imaged in Hare et al. (2019). This wide distribution of propagation speeds strongly implies that needles have a wide variety of conductivity when they twinkle. Some needles are poorly conducting, and so the twinkle propagates slowly like a stepped leader, and some needles are more conducting and so the twinkles propagate more like recoil leaders. We have seen, in Figure 3, that twinkles can slow down as they propagate. An obvious possible explanation is that the electric field decreases in amplitude further from the needle. If the corona-sheath effect is significant than it is even possible that the electric field near the leader could point toward the leader, but at a further radial distance the electric field could point away from the channel again (as shown in Figure 25).

The hypothesis that needles have different temperatures when they twinkle, which results in a range of twinkle propagation behaviors, is consistent across all our observations. For example, in Figure 2, it is clear that the different needle twinkles have different VHF source densities. Figure 15 shows that the imaged density of VHF sources weakly correlates with twinkle speed. Figures 10 and 11 show that the first and last VHF emissions of each twinkle are not all in similar locations. This raises the distinct possibility that needle twinkles can propagate without emitting mappable VHF radiation.

The fact that needles at least sometimes step, as indicated by the distribution of time differences between sources in Figure 16, may seem contradictory to the possibility of the needle remaining conducting between twinkles. However, due to the fact that faster twinkles have fewer located VHF sources we have been unable to extract how twinkle stepping behavior relates to twinkle propagation speed. Analogous to dart and dart-stepped leaders, our hypothesis that the range of twinkle propagation behavior is due to a wide range of conductivity would predict that twinkles propagate faster if the needle is more conducting and thus should show less (or no) stepping behavior, whereas the slower propagating needles should exhibit significantly more stepping.

There seems to be a very strong limit on the length of needles, as we have observed very few longer than 100 m. The physical reason for this limit is not at all clear. Saba et al. (2020) showed that needles occur at the locations of corona-brush splits, and so we guess that the length of needles is related to the size of the corona at the tip of the leader, but such a hypothesis is very difficult to test.

3.4. The Silence of the Positive Leaders

Hare et al. (2019) noted that we are not able to image tip of the positive leader in VHF. The natural question that arises is, is it possible to set an upper limit on the VHF power emitted by the positive leader. In this study, we noted that after the return stroke of the 2017 flash we did not receive any VHF radiation for almost a millisecond. Furthermore, after the return stroke the needle production head jumps forward by 250 m, consistent with continuous silent propagation of the positive leader. Thus, under the assumption that the positive leader was propagating during the VHF silence after the return stroke, the VHF power density emitted by a positive leader, at about 10 km distant, must be less than our background noise power, which is dominated by the galactic background, at about 1×10^{-12} W (Hare et al., 2020). Thus,

$$\frac{P_{Lemitted}}{R^2} A < P_{Greceived}, \quad (2)$$

where $P_{Lemitted}$ is the power emitted by the positive leader, R is the distance between the closest antenna and the positive leader (≈ 8 km), A is the effective area of our antennas (≈ 1 m²), and $P_{Greceived}$ is the received galactic background power. Therefore, $P_{Lemitted} < 7 \times 10^{-5}$ W, in our 30–80 MHz frequency range, under our assumption that the positive leader was indeed propagating. For comparison, we have observed that the largest radio pulses we received from negative leaders have a peak power with an order-of-magnitude of 4 kW, emitted in 10-ns wide pulses of 40 μ J. Note, here, we discuss peak power, not average, since it is peak power that determines if we can see a VHF source without beam-forming.

4. Conclusions

In this study, we have presented detailed observations of needles imaged in VHF. Including the distributions of times between twinkles, VHF lengths, and twinkle propagation speeds. We have observed that:

1. the time between needle twinkles increases over time (Saba et al., 2020)
2. needle width is smaller than our meter-scale spatial resolution
3. twinkle propagation speed can range from 10^5 up to 10^7 m/s
4. some twinkles start propagating fast and slow down
5. faster twinkles have fewer located VHF sources
6. some twinkles show signs of stepping
7. recoil leaders and return strokes quench needle activity
8. needle activity can occur over a long span (>3 km) of the positive leader
9. nearby needles do not twinkle in-sync, and can even twinkle at different rates

We have explored in detail possibilities for how the electric field perpendicular to the channel could reverse direction, including the three possibilities presented by Hare et al. (2019): disconnection hypothesis, propagation-induced field reversal, and recoil leaders. The disconnection hypothesis is that if the positive leader becomes highly resistive than it could gain a more negative potential than the ambient field. This hypothesis describes the interactions between recoil leaders and needles very well, and could result in relatively uniform needle activity along the positive leader as is observed. We have also discussed the corona-sheath effect, where negative charge accumulation on the leader channel can result in a complex field configuration, including field reversal close to the channel. This will happen behind the tip of a propagating leader, which we call propagation-induced field reversal. Propagation-induced field reversal can explain needle activity on well-conducting leader channels, but it only results in needle activity very close to the leader tip. Furthermore, since the first twinkle of a needle will discharge the corona sheath around a needle, it is not clear how the corona sheath could play an important role in subsequent twinkles. Finally, we have discussed the possibility that current pulses on the leader channel, like recoil leaders could initiate needle twinkles, but we have not found any additional evidence other than the one case presented in Hare et al. (2019, Supplementary Material), and it is inconsistent with the majority of needle twinkles that we observe.

We have concluded that because needle twinkles have such a wide variety of speeds and VHF structure, then they likely have a wide variety of propagation mechanisms, ranging from twinkles that act like step leaders up to twinkles that propagate like dart leaders. This implies the strong possibility that needle twinkles can propagate without emitting VHF, and that this range of phenomena could be due to the temperature of the needle at the time of each twinkle.

Data Availability Statement

The data are available from the LOFAR LTA, see https://www.astron.nl/lofarwiki/doku.php?id=public:lta_howto (section “Staging Transient buffer Board (TBB) data”) for access. The file names of the two flashes are: L612746_D20170929T202255.000Z_“stat”_R000_tbb.h5 and L703974_D20190424T194432.504Z_“stat”_R000_tbb.h5. Both must have the prefix: [srm://srm.grid.sara.nl/pnfs/grid.sara.nl/data/lofar/ops/TBB/lightning/](https://srm.grid.sara.nl/pnfs/grid.sara.nl/data/lofar/ops/TBB/lightning/) and “stat” should be replaced with the station name: CS001, CS002, CS003, CS004, CS005, CS006, CS007, CS011, CS013, C017, CS021, CS024, CS026, CS028, CS030, CS031, CS032, CS101, CS104, RS106, CS201, RS205, RS208, RS210, CS301, CS302, RS305, RS306, RS307, RS310, CS401, RS406, RS407, RS409, CS501, RS503, RS508, or RS509.

References

- Dwyer, J. R., & Uman, M. A. (2014). The physics of lightning. *Physics Reports*, 534(4), 147–241. <https://doi.org/10.1016/j.physrep.2013.09.004>
- Edens, H. E., Eack, K. B., Eastvedt, E. M., Trueblood, J. J., Winn, W. P., Krehbiel, P. R., & Thomas, R. J. (2012). VHF lightning mapping observations of a triggered lightning flash. *Geophysical Research Letters*, 39, L19807. <https://doi.org/10.1029/2012GL053666>
- Hare, B. M., Scholten, O., Dwyer, J., Ebert, U., Nijdam, S., Bonardi, A., & Winchen, T. (2020). Radio emission reveals inner meter-scale structure of negative lightning leader steps. *Physical Review Letters*, 124, 105101. <https://doi.org/10.1103/PhysRevLett.124.105101>
- Hare, B. M., Scholten, O., Dwyer, J., Trinh, T. N. G., Buitink, S., ter Veen, S., et al. (2019). Needle-like structures discovered on positively charged lightning branches. *Nature*, 568, 360–363. <https://doi.org/10.1038/s41586-019-1086-6>

Acknowledgments

The LOFAR cosmic-ray key science project acknowledges funding from an Advanced Grant of the European Research Council (FP/2007-2013)/ERC Grant Agreement 227610. The project has also received funding from the European Research Council (ERC) under the European Union’s Horizon 2020 research and innovation programme (Grant Agreement 640130). We further acknowledge financial support from FOM (FOM-project 12PR304). S. ter Veen acknowledges funding from the Khalifa University Startup grant (project code 8474000237). B. M. Hare was supported by the NWO (VI.VENI.192.071). K. Mulrey was supported by FWO (FWO-12ZD920N). A. Nelles acknowledges the DFG Grant NE 2031/2-1. T. N. G. Trinh acknowledges funding from the Vietnam National Foundation for Science and Technology Development (NAFOSTED) under (Grant 103.01-2019.378). LOFAR, the Low Frequency Array designed and constructed by ASTRON, has facilities in several countries, that are owned by various parties (each with their own funding sources), and that are collectively operated by the International LOFAR Telescope foundation under a joint scientific policy.

- Li, S., Qiu, S., Shi, L., & Li, Y. (2020). Broadband VHF observations of two natural positive cloud-to-ground lightning flashes. *Geophysical Research Letters*, *47*, e2019GL086915. <https://doi.org/10.1029/2019GL086915>
- Malagón-Romero, A., & Luque, A. (2019). Spontaneous emergence of space stems ahead of negative leaders in lightning and long sparks. *Geophysical Research Letters*, *46*, 4029–4038. <https://doi.org/10.1029/2019GL082063>
- Maslowski, G., & Rakov, V. A. (2009). New insights into lightning return-stroke models with specified longitudinal current distribution. *IEEE Transactions on Electromagnetic Compatibility*, *51*(3), 471–478. <https://doi.org/10.1109/TEMC.2009.2017200>
- Pu, Y., & Cummer, S. A. (2019). Needles and lightning leader dynamics imaged with 100–200 MHz broadband VHF interferometry. *Geophysical Research Letters*, *46*, 13556–13563. <https://doi.org/10.1029/2019GL085635>
- Saba, M., de Paiva, A., & Concollato, L. (2020). Optical observation of needles in upward lightning flashes. *Scientific Reports*, *10*, 17460. <https://doi.org/10.1038/s41598-020-74597-6>
- Scholten, O., Hare, B. M., Dwyer, J., Sterpka, C., Kolmaov, O., Santolik, O., et al. (2020). The initial stage of cloud lightning imaged in high-resolution. *Journal of Geophysical Research: Atmospheres*, *126*, e2020JD033126. <https://doi.org/10.1002/essoar.10503153.1>
- Shao, X. M., & Krehbiel, P. R. (1996). The spatial and temporal development of intracloud lightning. *Journal of Geophysical Research*, *101*(D21), 26641–26668. <https://doi.org/10.1029/96JD01803>
- Shao, X. M., Rhodes, C. T., & Holden, D. N. (1999). Rf radiation observations of positive cloud-to-ground flashes. *Journal of Geophysical Research*, *104*(D8), 9601–9608. <https://doi.org/10.1029/1999JD900036>
- van Haarlem, M. P., Wise, M. W., Gunst, A. W., Heald, G., McKean, J. P., Hessels, J. W. T., et al. (2013). LOFAR: The LOW-Frequency ARray. *Astronomy and Astrophysics*, *556*, A2. <https://doi.org/10.1051/0004-6361/201220873>
- Warner, T. A., Saba, M. M. F., Schumann, C., Helsdon, J. H. Jr., & Orville, R. E. (2016). Observations of bidirectional lightning leader initiation and development near positive leader channels. *Journal of Geophysical Research: Atmospheres*, *121*, 9251–9260. <https://doi.org/10.1002/2016JD025365>
- Yuan, S., Jiang, R., Qie, X., Sun, Z., Wang, D., & Srivastava, A. (2019). Development of side bidirectional leader and its effect on channel branching of the progressing positive leader of lightning. *Geophysical Research Letters*, *46*, 1746–1753. <https://doi.org/10.1029/2018GL080718>